ISSN 1807-1929
Revista Brasileira de Engenharia Agrícola e Ambiental
Brazilian Journal of Agricultural and Environmental Engineering
v.30, n.1, e291614, 2026
Campina Grande, PB – http://www.agriambi.com.br – http://www.scielo.br/rbeaa

Original Article

Origin and hydrogeochemical processes in the salinization of a coastal aquifer in the Colombian Caribbean[1]

Origem e processos hidrogeoquímicos na salinização de um aquífero costeiro no Caribe colombiano

Zoraya Y. Martínez Lara[2*], Mónica C. Cantero Benitez[2], Adriana S. Raciny Soto[2], Neider A. Burgos Ortiz[2] & Ángela I. Villalba López[2]

[1] Research developed at Universidad de Córdoba, Campus Central, Montería, Córdoba, Colombia
[2] Universidad de Córdoba/Departamento de Ingeniería Ambiental/Grupo de Investigación GIMESA, Montería, Córdoba, Colombia

HIGHLIGHTS:

Brines are mainly distributed in the northern and northeastern sectors of the Lower Sinú floodplain.
The variables with the highest degree of association in the hydrogeological system are Na^+, Cl^- and electrical conductivity.
Agrochemical use in crops increases Na^+, Cl^-, and K^+ concentrations in the Lower Sinú aquifer.

ABSTRACT: Coastal aquifers are affected by various processes that control the complex dynamics of salinization, such as the case of the coastal unconfined aquifer of the deltaic zone of the Sinú River, located around the Lower Sinú Coastal Zone in the Colombian Caribbean. In this fluvial-marine plain system, soil and groundwater salinization seriously limit the economic development supported by agriculture and ecosystem services. This study aims to characterize the origin of the hydrogeochemical processes and the major ions that control salinization in the local shallow alluvial aquifer. Using a combined approach of hydrogeochemical techniques and multivariate statistical analysis, 388 samples were collected from a monitoring database, between 2002 and 2008, and analyzed. Major ion concentrations (Cl^-, HCO_3^-, SO_4^{2-}, Na^+, K^+, Mg^{2+}, Ca^{2+}), total dissolved solids (TDS), electrical conductivity (EC), pH, and distance to the coastline were evaluated. The results reveal two distinct groups of groundwater flows, differentiated by ion concentrations, salinity levels, and statistical correlations between the ions. A total of twenty five hydrochemical facies were identified, with Na–Cl, MixNa–Cl, MixMg–Cl, and Mg–Cl being the most dominant. The spatial distribution of these facies suggests a strong influence of both natural and anthropogenic factors. The origin of the ions varies among marine, lithological, and meteoric sources. The main hydrogeochemical processes responsible for mineralization include seawater intrusion and ion exchange reactions. These findings are essential for improving groundwater management strategies and mitigating salinization in vulnerable coastal environments.

Key words: unconfined aquifers, groundwater salinization, multivariate statistics, hydrochemical diagrams

RESUMO: Aqüíferos costeiros são afetados por diversos processos que controlam a complexa dinâmica da salinização, como é o caso do aquífero costeiro livre da zona deltaica do rio Sinú, localizado na Zona Costeira do Baixo Sinú, no Caribe colombiano. Neste sistema de planície fluviomarinha, a salinização do solo e da água subterrânea limita seriamente o desenvolvimento econômico baseado na agricultura e nos serviços ecossistêmicos. Este estudo tem como objetivo caracterizar a origem dos processos hidrogeoquímicos e dos principais íons que controlam a salinização no aquífero aluvial raso local. Utilizando uma abordagem combinada de técnicas hidrogeoquímicas e análise estatística multivariada, foram analisadas 388 amostras de um banco de dados de monitoramento coletado entre 2002 e 2008. Foram avaliadas as concentrações dos principais íons (Cl^-, HCO_3^-, SO_4^{2-}, Na^+, K^+, Mg^{2+}, Ca^{2+}), os sólidos totais dissolvidos (STD), a condutividade elétrica (CE), o pH e a distância da linha costeira. Os resultados revelam dois grupos distintos de fluxos de água subterrânea, diferenciados pelas concentrações de íons, níveis de salinidade e correlações estatísticas entre os íons. Foram identificadas vinte e cinco fácies hidrogeoquímicas, sendo os Na–Cl, MixNa–Cl, MixMg–Cl e Mg–Cl as mais dominantes. A distribuição espacial dessas fácies sugere uma forte influência de fatores tanto naturais quanto antrópicos. A origem dos íons varia entre fontes marinhas, litológicas e meteóricas. Os principais processos hidrogeoquímicos responsáveis pela mineralização incluem a intrusão de água do mar e as reações de troca iônica. Esses achados são fundamentais para aprimorar as estratégias de gestão da água subterrânea e mitigar a salinização em ambientes costeiros vulneráveis.

Palavras-chave: aquíferos livres, salinização da água subterrânea, estatística multivariada, diagramas hidroquímicos

• Ref. 291614 – Received 03 Nov, 2024
* Corresponding author - E-mail: zorayamartinez26@gmail.com
• Accepted 20 Jul, 2025 • Published 07 Aug, 2025
Editors: Antônio Gustavo de Luna Souto & Hans Raj Gheyi

Introduction

In Colombia, extensive areas of soil with high agricultural and ecological value have been severely affected by salinization, resulting in the progressive degradation of their productive and conservation capacity (Narváez et al., 2014; González-Pedraza et al., 2022). This process represents a critical environmental challenge in the fluvial-marine plain of the Sinú River, where the accumulation of salts in surface layers and shallow soil profiles (just a few centimeters thick) reduces crop yields and threatens food security and ecosystem integrity (Combatt et al., 2015; González-Pedraza et al., 2022).

Previous studies in the Lower Sinú delta have shown that marine intrusion intensifies during the dry season, as a result of reduced river discharge and greater tidal influence. Modeling results indicate that the marine wedge can extend up to 3 km inland through the Mireya and Medio distributaries—both branches of the Sinú River—with salinity values reaching 28-35 ppt approximately 2 km upstream (Torres-Bejarano et al., 2023). Groundwater studies report similarly elevated salinity levels in this same deltaic sector during dry periods, primarily due to marine intrusion and increased evaporation under low-flow conditions (Narváez et al., 2014). This seasonal salinization pattern correlates with high concentrations of chloride, sodium, and magnesium ions, reflecting the influence of seawater intrusion facilitated by diminished fluvial input (Narváez et al., 2014; Combatt et al., 2015). Marine intrusion is widely recognized as being the dominant driver of groundwater and soil salinization in this coastal plain (Mercado-Fernández et al., 2011; Narváez et al., 2014; Combatt et al., 2015).

Understanding the mechanisms that control salinization is fundamental to the design of sustainable groundwater management strategies in vulnerable coastal systems (Sunkari et al., 2022; Tajwar et al., 2025). Various approaches are used in hydrogeological studies. These include the integrated use of hydrogeochemical and statistical methods and techniques, such as molar ratio in bivariate plots (Abu-Alnaeem et al., 2018; Gaikwad et al., 2022) and multivariate statistical techniques in cluster analyses (El Yousfi et al., 2022). The synergistic application of these methods has been successful in evaluating the origin, processes, and degree of evolution of the problems associated with the increase in salts and contaminants present in aquifer systems (INGEOMINAS, 2004; Salem et al., 2021).

Considering the growing concern over salinization in coastal groundwater systems, this study aims to contribute to the elucidation of the factors and processes that drive salinity in the unconfined aquifer of a sector within the Lower Sinú Coastal Zone. By employing an integrated approach that combines hydrogeochemical analysis with multivariate statistical techniques, the research focuses on the characterization of hydrochemical facies, the identification of salinity sources, and the evaluation of the dominant geochemical processes responsible for groundwater mineralization.

Material and Methods

This study was carried out on the alluvial plain and marshes of the lower course of the Sinú River in the Colombian Caribbean, covering an area of 3,109.4 ha (Figure 1). Groundwater samples were collected from 25 piezometers located in the floodplain sector with the highest evidence of salinization, whose locations are detailed in Table 1.

The study area is part of the Sinú Belt, located in the western part of the Department of Córdoba, a structural region formed by the emplacement of accretion prisms towards the continent

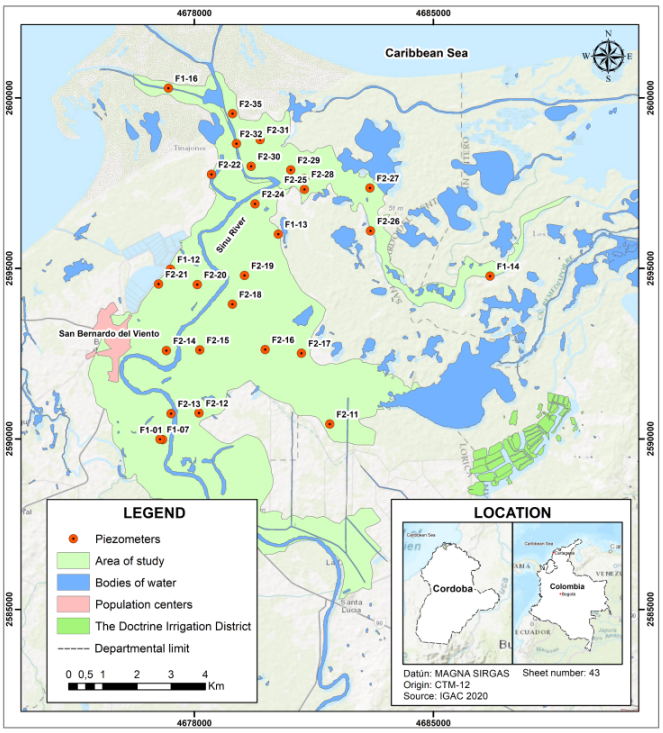

Figure 1. Location of the study area

Table 1. Georeferenced locations of piezometers in the Lower Sinú aquifer. WGS 1984 Coordinate System

ID	N	W
F1-01	9° 19' 36.901"	75° 56' 26.200"
F1-07	9° 19' 37.247"	75° 56' 28.680"
F1-12	9° 22' 19.602"	75° 56' 19.926"
F1-13	9° 22' 53.991"	75° 54' 36.977"
F1-14	9° 22' 15.517"	75° 51' 13.497"
F1-16	9° 25' 12.210"	75° 56' 23.476"
F2-11	9° 19' 53.058"	75° 53' 46.169"
F2-12	9° 20' 02.660"	75° 55' 51.581"
F2-13	9° 20' 01.725"	75° 56' 18.318"
F2-14	9° 21' 01.996"	75° 56' 23.264"
F2-15	9° 21' 00.553"	75° 54' 13.705"
F2-16	9° 21' 03.732"	75° 54' 48.656"
F2-17	9° 21' 02.915"	75° 55' 51.384"
F2-18	9° 21' 46.729"	75° 55' 20.391"
F2-19	9° 22' 14.266"	75° 55' 08.988"
F2-20	9° 22' 05.222"	75° 55' 54.265"
F2-21	9° 22' 05.341"	75° 56' 31.284"
F2-22	9° 23' 50.372"	75° 55' 41.578"
F2-24	9° 23' 22.660"	75° 54' 59.506"
F2-25	9° 23' 36.802"	75° 54' 12.153"
F2-26	9° 22' 57.781"	75° 53' 08.525"
F2-27	9° 23' 38.634"	75° 53' 09.414"
F2-28	9° 23' 47.014"	75° 54' 12.118"
F2-29	9° 23' 55.228"	75° 54' 25.459"
F2-30	9° 23' 58.418"	75° 55' 03.500"
F2-31	9° 24' 23.9226"	75° 54' 55.188"
F2-32	9° 24' 19.911"	75°55' 17.827"
F2-35	9° 24' 48.520"	75° 55' 21.846"

during the Cenozoic (INGEOMINAS, 2004). Lithologically, it is composed of Quaternary deposits of diverse granulometries and origins, being clayey in the basins of the Sinú River and the marshes of Cispatá Bay but sandy clay in the Sinú dikes, beach areas, and accumulation terraces. The geomorphology of the study area is characterized by the presence of marine and fluvial plains, which were shaped by geological proccesses active from the Holocene to the present (INGEOMINAS, 2004).

The region experiences a unimodal rainfall regime, characterized by three distinct climatic periods. The dry season extends from December to April and is marked by mininal precipitation, typically less than 50 mm per month. The transitional season occurs between May and July and is defined by sporadic rainfall, with monthly totals not surpassing 120 mm. The wet season, from August to November, is characterized by more intense rainfall, with values reaching up to 270 mm per month (IGAC, 2009).

The average air temperature registers the highest values in the transitional period in May (29.0-33.0 °C) and the lowest in October (27.9 °C), in the wet season; the dry season registers intermediate values with averages of 26.7-28.0 °C. At a regional level, the area is considered to be a hydrogeological unit characterized as a complex of unconsolidated deposits of lacustrine, deltaic, and marine environments that form aquifers of very low yield (INGEOMINAS, 2004).

The hydrochemical database used was collected between the years 2002 and 2008 (Bustamante-Barrera & Cantero-Benitez, 2006; Combatt et al., 2015) and presents a record of the parameters: pH, electrical conductivity (EC, in dS m^{-1}), total dissolved solids (TDS, in g L^{-1}), the soluble cations of calcium, magnesium, sodium, and potassium (Ca^{2+}, Mg^{2+}, Na^{+}, and K^{+}, respectively, in mEq L^{-1}), and soluble anions chlorides, sulfates, and bicarbonates (Cl^{-}, SO_4^{2-}, and HCO_3^{-}, respectively, in mEq L^{-1}). A total of 388 groundwater samples were analyzed, following the standard procedures of the IGAC (2006). All analyses were checked for electrical charge imbalances, which, in all cases, were less than 10%. Anion and cation percentages were calculated with respect to the sum of anions and cations, respectively (in mEq L^{-1}). Additionally, the distance between the piezometers and the coastline (km) was integrated into the analysis: a parameter called 'DIST'.

A hierarchical agglomerative method was applied to the data population, grouping it by observations to delimit hydrochemically homogeneous water groups. The data were standardized using the minimum variance criterion or Ward method and the squared Euclidean distance metric (Sangadi et al., 2022) in the Statgraphics 19 - X64 software. The number of clusters was selected using the agglomeration distance criterion (François et al., 2017). Cluster analysis is a technique for grouping similar components and identifying differences between elements.

Once the number of clusters or groups was established, their descriptive statistics, and the associations of the variables, were analyzed using Spearman's rank correlation. This information supported the analysis of the origin of the ions and the relationships between analytes in the water groups (Tajwar et al., 2025). The Spearman correlation coefficient (Eq.1) was calculated at a significance level of 5% of probability. Based on the magnitude of R, three categories of association were defined: strong (R > 0.80), moderate (0.50 < R ≤ 0.80) and weak (R ≤ 0.50) (Bauer et al., 2022; Das et al., 2022).

$$R = 1 - \frac{6\sum d_i^2}{n\left(n^2 - 1\right)} \quad (1)$$

where:

n - quantity of data being classified;

d_i - difference between xi-yi;

xi - ranges of data i with respect to a variable; and,

yi - range of data i with respect to a second variable.

The hydrogeochemical facies were interpreted using the Piper diagram modified by Kelly (Kelly, 2006; El Yousfi et al., 2022; Tajwar et al., 2025), which allows the characterization of groundwater samples into chemical families with similar signatures to identify the origin of the flows. The Gibbs and Chadha diagrams and bivariate graphs were used to describe the mechanisms and sources of the ions that favor the mineralization of water in the hydrogeological system (Abu-Alnaeem et al., 2018; Bauer et al., 2022; El Yousfi et al., 2022; Gaikwad et al., 2022); the Gibbs diagram was interpreted based on the modifications of Marandi & Shand (2018). The following hydrogeochemical processes were interpreted using bivariate plots: cation exchange through the ratio (Ca^{2+} + Mg^{2+} - HCO_3^{-} - SO_4^{2-}) vs. (Na^{+} + K^{+} - Cl^{-}); evaporation, halite dissolution and anthropogenic activities through the (Na^{+}/Cl^{-}) vs EC ratio; and marine intrusion according to the $Cl^{-}/(Cl^{-}$ + HCO_3^{-}) ratio (also called the Simpson ratio (rS)). According to the rS, groundwaters can be classified as follows: normal water without contamination (rS < 1), slightly contaminated water (1 ≤ rS ≤ 2), moderately contaminated water (2 < rS ≤ 6), seriously contaminated water (6 < rS ≤ 15), and highly contaminated water (rS >15).

Results and Discussion

The dendrogram of observations revealed the existence of two groups, or clusters, of groundwater at a 4000 Euclidean distance (Figure 2). The parameters of the mean, standard deviation, and coefficient of variation of the most critical chemical variables are listed in Table 2 for the water groups and the data population. On average, the data population reports flows which are slightly alkaline pH (z = 7.57), strongly saline EC (x = 10.02 dS m^{-1}), and with very high TDS (x = 6,635 mg L^{-1}). With the exception of pH and HCO_3^{-}, the variables presented high standard deviations, evidencing a high variability in ionic concentration. High coefficients of variation in Cl^{-}, Na^{+}, K^{+}, Mg^{2+}, and SO_4^{2-} concentrations in groundwater are commonly associated with multiple overlapping processes, including agricultural inputs, wastewater infiltration, ion exchange reactions, and the dissolution of evaporitic minerals such as halite and gypsum. These mechanisms contribute to spatial and temporal heterogeneity in aquifer geochemistry, especially in coastal or semi-arid regions with variable hydrogeological conditions (Tajwar et al., 2025).

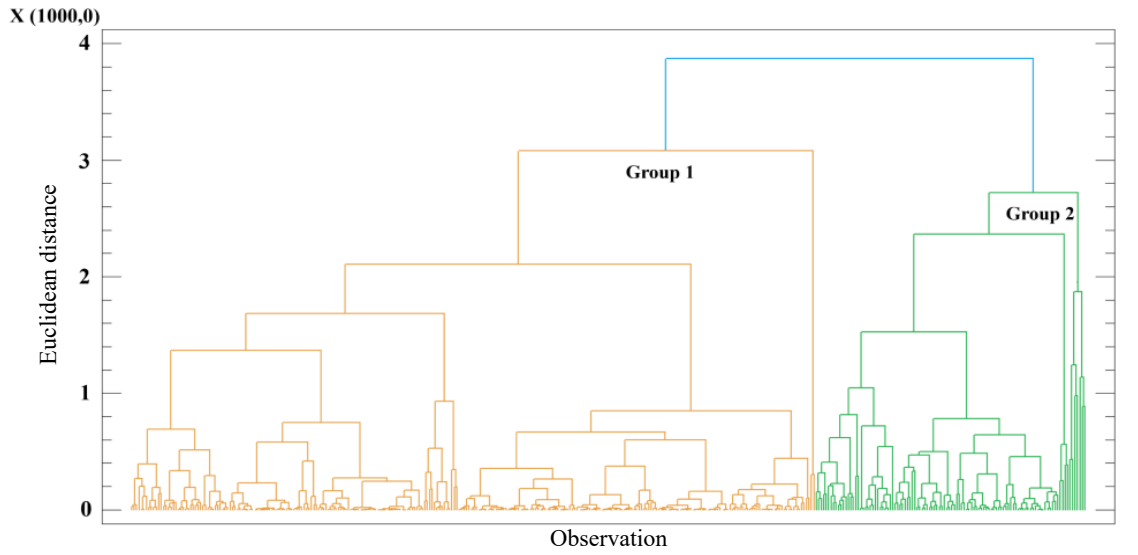

Figure 2. Dendrogram displaying the hierarchical clustering of 388 groundwater samples collected in the Lower Sinú, Coastal Zone, Córdoba, Colombia

Table 2. Descriptive statistics of hydrochemical parameters in Groups 1 and 2 and the overall Population

Parameters	Group 1 (n=269)					Group 2 (n=119)					Population (n=388)				
	$\bar{x}$	SD	CV (%)	Min	Max	$\bar{x}$	SD	CV (%)	Min	Max	$\bar{x}$	SD	CV (%)	Min	Max
pH	7.6	0.7	9	4.9	9.1	7.4	0.6	8.3	5.97	8.79	7.57	0.67	8.9	4.9	9.1
Ca^{2+}	5.3	5.4	101.8	0.2	26	24.8	16.2	65.3	0.8	82	11.27	13.45	119.5	0.2	82
Mg^{2+}	11.3	12	105.9	0.3	96	53.5	54.1	101.2	1.3	420	24.24	37.03	152.8	0.3	420
Na^{+}	30.4	39.1	128.7	0.06	268.6	129.1	108.5	84.1	0.12	679	60.66	82.01	135.2	0.06	679
K^{+}	1.4	3.6	263.3	0	32.87	3.9	9.9	253.3	0.02	66.43	2.14	6.32	295.0	0.003	66.43
HCO_3^{-}	6	4.8	80.1	0.6	32	5.2	3.4	65.3	1	16.5	5.78	4.44	77.0	0.6	32
Cl^{-}	35.2	43.9	124.7	0	6	170.9	99.4	58.1	0	10.8	76.79	90.94	118.4	0	10.8
SO_4^{2-}	6.2	9.6	153.7	0.14	252	34.4	64.7	188.3	1.26	670.31	14.85	38.85	261.6	0.14	670.31
EC	4.4	4.6	104	0	67.2	22.6	50.6	223.5	0.17	482.44	10.02	29.437	293.7	0	482.44
TDS	3220.4	3618.7	112.4	0	22.4	14353	16483.5	114.8	0.0151	438	6634.7	10878.2	164.0	0.00162	438
DIST	4.7	1.8	38.7	0	21000	4.4	1.6	34.7	15.4	133080	4.6	1.8	37.6	0	133080

x - Mean; SD - Standard deviation; CV - Coefficient of variation; cations and anions units - mEq L^{-1}; TDS units - mg L^{-1}; EC units - dS m^{-1}

Although, for the groups and the population, the concentration of cations decreased according to the condition $Na^{+} > Mg^{2+} > Ca^{2+} > K^{+}$ and anions decreased according to the condition $Cl^{-} > SO_4^{2-} > HCO_3^{-}$, the fundamental difference between the groups is due to the value of the parameters measured. This is because, except for bicarbonate, the concentrations of ions and TDS were higher in Group 2 than in Group 1, a behavior also observed for electrical conductivity.

The data in Table 2 indicate that the mean groundwater flows in Group 1 (69%) exhibit ionic abundance, where $Cl^{-} > Na^{+} > Mg^{2+} > SO_4^{2-} > HCO_3^{-} > Ca^{2+} > K^{+}$; they are moderately saline, with high TDS and the lowest ionic concentrations. Group 2 (31%) reports groundwater where $Cl^{-} > Na^{+} > Mg^{2+} > SO_4^{2-} Ca^{2+} > HCO_3^{-} > K^{+}$; they are extremely saline, with critical TDS, and have the highest ion concentrations (Richards, 1954). In this group, except for bicarbonate, ionic concentrations increased relative to Group 1, by between 278% (K^{+}) and more than 400% (SO_4^{2-}, Cl^{-}, Mg^{2+}, Ca^{2+}, and Na^{+}).

The heatmap illustrates the ordinal correlations between variables by group (Figure 3). In Group 1, strong, positive,

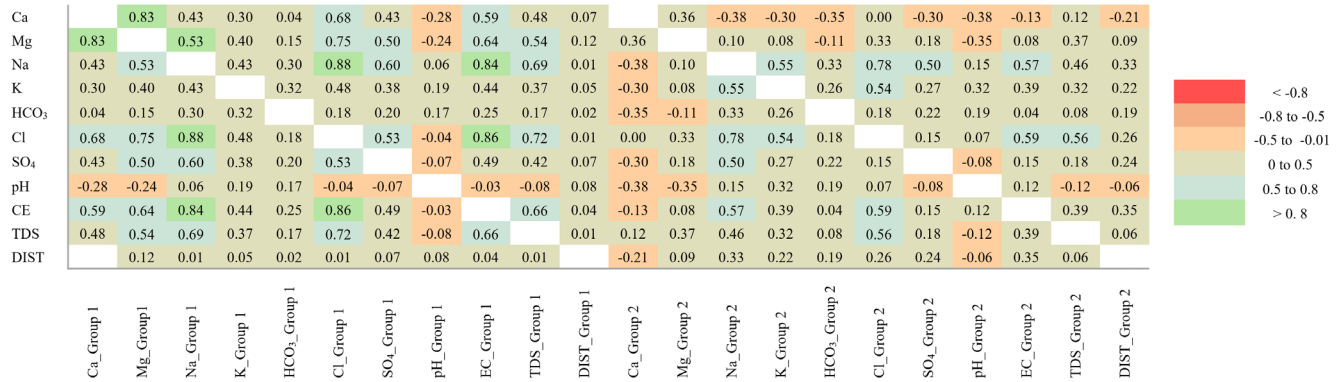

Figure 3. Correlation heatmap of the main chemical elements in 388 groundwater samples from Groups 1 and 2

and significant correlations (R > 0.80) were observed between conductivity and chloride (R = 0.90), conductivity and sodium (R > 0.80), and chloride and sodium (R > 0.80), reflecting the incidence of Na^+ and Cl^- ions in the increase of electrical conductivity and groundwater mineralization (Askri et al., 2022). In this group, the strong association between Ca^{2+} and Mg^{2+} also indicates a common origin (Osiakwan et al., 2021). In Group 2, Na^+ and Cl^- are the only parameters exhibiting a moderate correlation, suggesting a common source (Sunkari et al., 2022). However, their weak to absent association with Mg^{2+}, SO_4^{2-}, and electrical conductivity differentiates this group from Group 1 and does not indicate an exclusively marine origin (Telahigue et al., 2020; Tajwar et al., 2025). Notably, the samples in this group exhibit the highest concentrations of major ions, total dissolved solids, and EC. Considering the fact that the study area is part of an extensive irrigation and drainage district with high agricultural productivity, it is highly likely that the observed salinity is related to anthropogenic pollution, particularly from the intensive use of agrochemicals such as fertilizers and pesticides (Telahigue et al., 2020; Sunkari et al., 2022).

In coastal areas, groundwater salinization is strongly influenced by anthropogenic activities, in addition to natural processes. Telahigue et al. (2020) noted that urban development, the use of fertilizers, and non-sealed septic tanks contribute significantly to increased salinity through the input of Cl^-, Na^+, and other ions. Abu-Alnaeem et al. (2018) observed that groundwater types reflect both natural conditions and human impacts, such as irrigation and land use. According to Sunkari et al. (2022), high EC values are linked to marine intrusion and human-induced sources, such as aquaculture and poor waste disposal.

The chemical composition of groundwater flows is influenced by variables such as CO_2 pressure, precipitation, the influence of marine aerosols, sea level rise, the presence of surface flows, geological characteristics of the aquifer, depth of the aquifer levels and anthropogenic inputs (Xu et al., 2021; Tajwar et al., 2025). High concentrations of Na^+ and Cl^-, dominant Na - Cl hydrochemical facies, and high variability in the investigated parameters are common behaviors in coastal aquifers (Sangadi et al., 2022). These characteristics are present in the Lower Sinú and have also been described in the coastal areas of Ghana, South Africa, Palestine, Italy, Bangladesh, Saudi Arabia, and Tunisia (Osiakwan et al., 2021). The neutral to alkaline pH and the abundance of Na^+ as the dominant cation in the Lower Sinú Coastal are similar to those reported for the shallow aquifer of the central sector of the Nile Delta (Salem et al., 2021), the southern Mekong Delta (Bauer et al., 2022), and the coastal region of Andhra Pradesh in India (Sangadi et al., 2022). However, in these aquifers, the average concentration of major ions and salinity (by TDS and EC) were lower than those reported for the Lower Sinú. This difference is primarily attributed to reduced freshwater recharge and the predominance of clayey alluvial deposits. In contrast, the lower salinity levels in the Nile, Mekong, and Andhra Pradesh deltas are associated with natural controls on the shallow aquifers, including surface hydrochemical processes and more effective recharge due to the notable presence of sandy and gravelly alluvial deposits.

The primary origin of chloride and sodium ions is a marine environment. These ions showed strong and positive correlations (0.77 to 0.92) for all periods and water groups, which is an expected pattern in coastal aquifers (Salem et al., 2021). Correlations close to 0.9 are usually observed between ions of marine origin (Cl^-, Na^+, Mg^{2+}, and SO_4^{2-}) and the salinity parameters EC and TDS, mainly when marine intrusion controls groundwater mineralization (Xu et al., 2021; Bauer et al., 2022). However, in the Lower Sinú, moderate to weak correlations were reported between some of the marine ions and the EC and TDS, indicating that the sources of the ions are diverse.

Figures 4 and 5 show the hydrochemical facies and their spatial distribution, based on the analysis of the Piper diagram

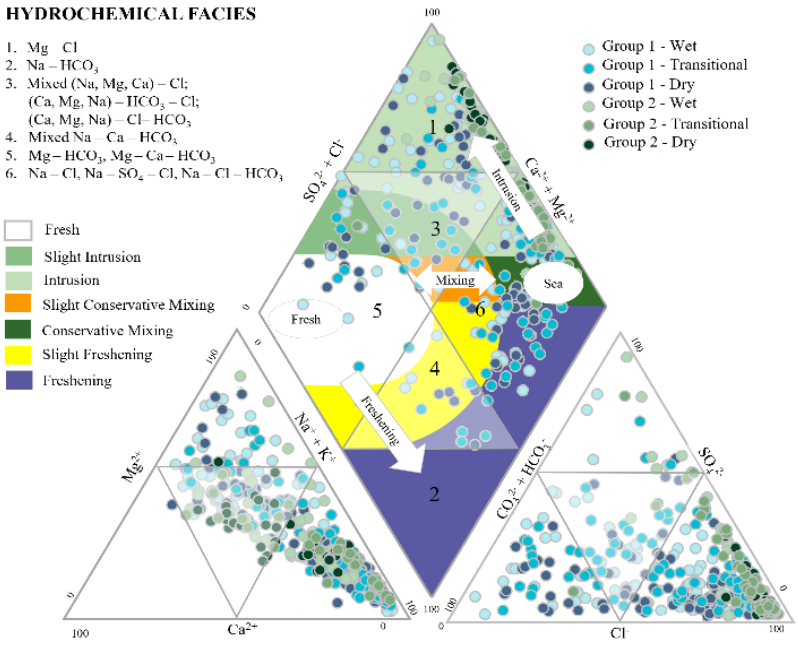

Figure 4. Hydrochemical facies by group and season in 388 groundwater samples from the unconfined Lower Sinú aquifer based on the Piper and Kelly diagrams

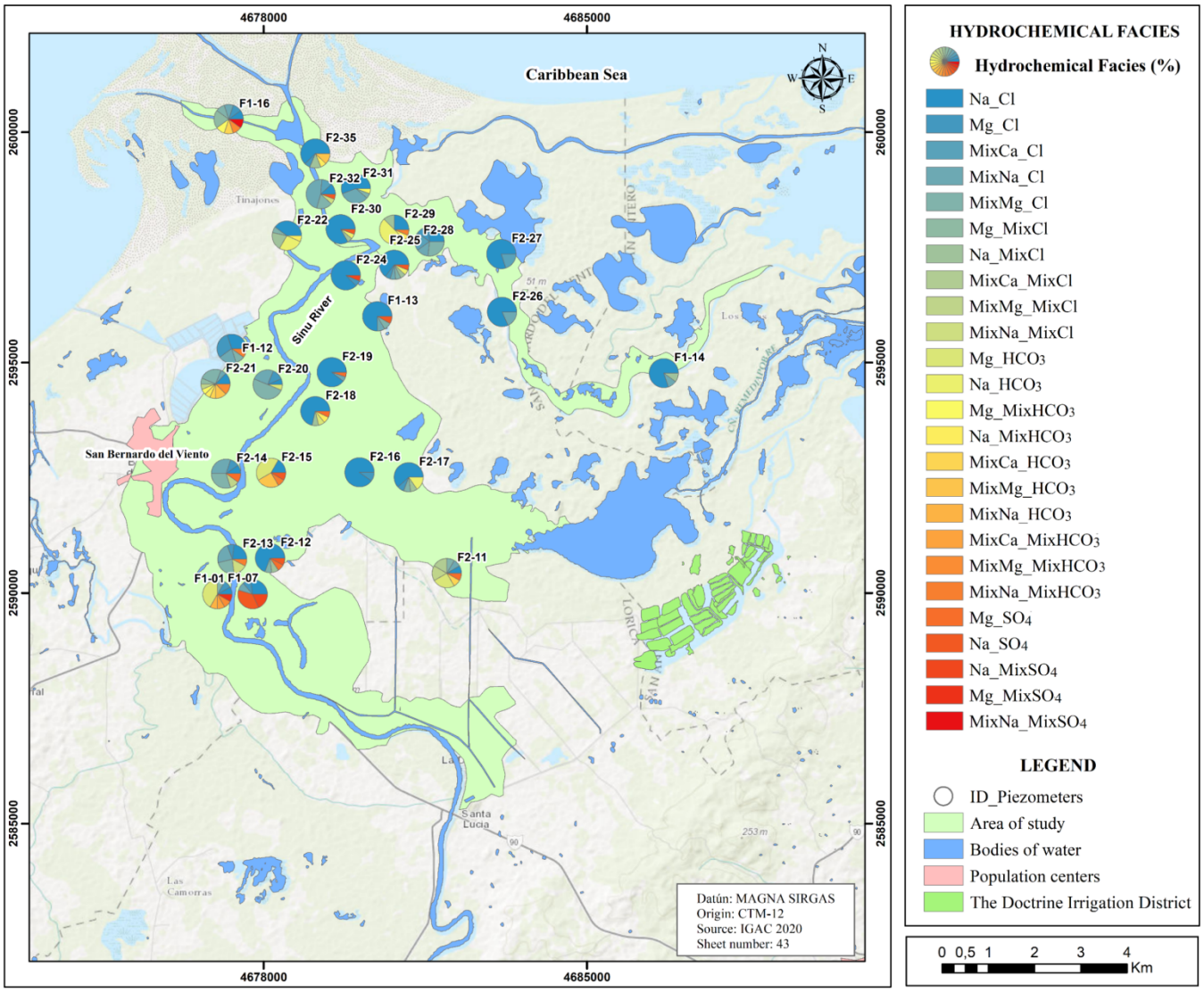

Figure 5. Spatial distribution of hydrochemical facies by group and season in 388 groundwater samples from the unconfined Lower Sinú aquifer

and the hydrochemical facies map (Telahigue et al., 2020). The dominant facies across the study area are sodium chloride (54.63%), magnesium chloride to sulfate (20.40%), and mixed cation-anion types (16.50%) (Figure 4).

The spatial distribution of hydrochemical facies in groundwater flows, as recorded in each piezometer, is presented in Figure 5. While Na-Cl facies clearly dominate the study area, several piezometers show less chlorinated water types, including mixed bicarbonate to sulfate facies, distributed throughout the study area. These comparatively fresher signatures are observed in the north and northwest sectors (F1-16, F2-29, F2-22), including parts of the Tinajones delta (e.g., F1-16) along the Corea distributary. Similar facies also appear in the central (F2-21, F2-15) and southern (F1-01, F1-07) portions of the plain, on both margins of the river. The piezometers most influenced by salinity are located in the northern part and on the right-hand margin of the current floodplain, at least 3 km inland from the coastline. These include sites near the Tinajones delta (F2-31, F2-30), the paleochannel of Caño Grando (F2-27, F2-26, F1-14), near the active course of the Sinú River (F2-24), and in the central zone farther from the current channel (F2-19, F2-16, F2-17).

Concerning the periods of the hydrological year, the Na-Cl facies were abundant according to the sequence: transitional season > dry > wet. For the categories of highest salinity (extremely to strongly saline), the EC presented a predominance by period according to the succession: transitional season > dry > wet, and the TDS predominated in the hypercritical and critical classes according to the behavior: dry season > transitional > wet (Richards, 1954). Figure 4 records the diverse origins and processes in the groundwater flows: a marine origin is related to intrusion and light intrusion (58.20%); a climatic origin is associated with rainwater precipitation (1.20%); a conservative mixture to light conservative mixture accounts for 18.30%; and the water-rock (mineral) interaction, related to freshening and light freshening, accounts for 18.80% (Telahigue et al., 2020).

According to Figure 6, the Chadha diagram (Balasubramanian et al., 2022; El Yousfi et al., 2022) indicates that the processes that modify the groundwater chemistry are marine intrusion (54%), freshening by reverse cation exchange (34%), salinization by direct cation exchange (4.40%), and precipitation by fresh recharge water (7.70%). Most of the data in Group 2 are characterized by reporting chloride family flows

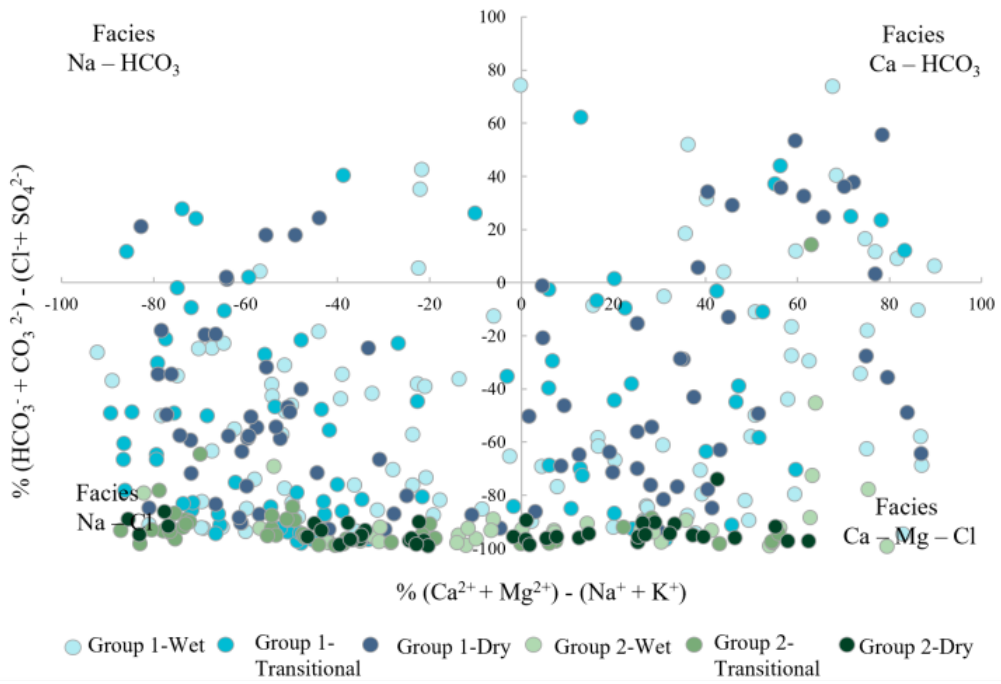

Figure 6. Chadha diagram by group and season for 388 groundwater samples from the unconfined Lower Sinú aquifer

with (HCO_3^-) - (Cl^- + SO_4^{2-}) of 80-100%, at points located at the graph's base.

The Gibbs diagram indicates a silicate-dominated system, where 70% of the samples have a Gibbs ratio of cations greater than 0.65 (Figure 7A). The brines located in the upper right part of the diagram (TDS > 10,000 ppm), represent 23% of the data, are hyperchlorinated, and exhibit values greater than 0.90 in the Gibbs ratio of the anions (Xu et al., 2021; Askri et al., 2022; El Yousfi et al., 2022).

The Gibbs diagram highlights salinization and freshening processes by ion exchange in the constitution of these flows (Figure 7A). A large percentage of brines (76.50%) correspond to groundwater from Group 2, while the remaining 23.5% belong to Group 1. Based on their occurrence throughout the hydrological year, brines were more prevalent during the dry season (41.20%), compared to the transitional (31.80%) and wet (27.10%) seasons. The spatial distribution of brines is closely associated with the most chlorinated hydrochemical facies identified in Figure 5. These facies are preferentially located in the northern and northeastern sectors of the alluvial plain, as well as along the right-hand bank of the Sinú River, which has been identified as the main discharge zone of the

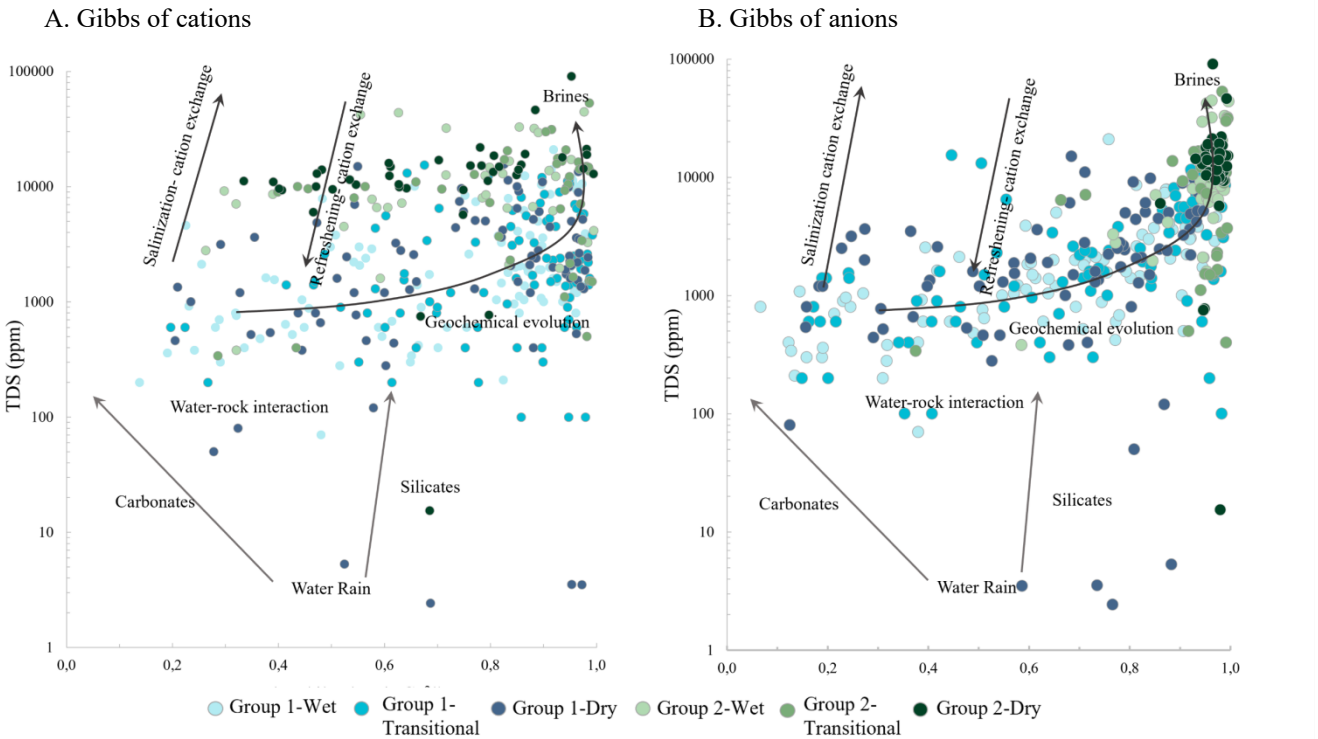

Figure 7. Gibbs diagrams for cations (A) and anions (B) by group and season for 388 groundwater samples from the unconfined Lower Sinú aquifer

aquifer system in previous studies (Mercado-Fernández et al., 2011). This pattern is consistent with the trends observed in the Gibbs diagrams for coastal aquifers undergoing progressive salinization (Abu-Alnaeem et al., 2018; Marandi & Shand, 2018; Gaikwad et al., 2022).

The geochemical evolution zone indicates the incidence of marine intrusion, conservative mixing, evaporite minerals dissolution and anthropogenic processes. According to the water concentration by TDS, this zone records 26.8% of the data as seawater (3000 < TDS < 10,000 ppm), 28.1% as brackish water (1000 < TDS < 3000 ppm), and 14% as freshwater (TDS < 1000 ppm).

Cation exchange-driven salinization and freshening processes account for approximately 48% of the samples represented in the cation Gibbs diagram (Figure 7A). These are characterized by cation ratios below 0.90 and TDS concentrations ≥ 1000 ppm. These processes are primarily associated with brackish water, seawater intrusion, and brine influence. In contrast, freshwater samples with TDS < 1000 ppm—classified as the least mineralized waters in the system (23.20%), according to Wang et al. (2022)—are mainly influenced by geochemical evolution processes (14%), silicate weathering due to rock/water interactions (5%), and direct meteoric precipitation (3%), as shown in Figure 7.

Fresh groundwaters with TDS <100 ppm reflect a meteoric origin and are characterized by low mineralization and suitability consumption. In the Lower Sinú, these flows are influenced by marine aerosols, as indicated by the dominance of Na-Cl, Na-HCO_3 and Mg-Na-Cl facies, and the ionic sequence $Cl^- > Na^+ > SO_4^{2-} > Mg^{2+}$ (Figure 7). The groundwater samples linked to meteoric precipitation processes are spatially distributed across the southern sector (F2-12, F2-13), the western limit and the left-hand bank of the river (F2-21, F2-22), the central plain (F2-18), and the northen and northeastern zones near Caño Grande, as well as the Tinajones delta (F2-27, F2-28, F2-29, F1-16). These patterns are consistent with previous findings in coastal aquifers, where early-stage groundwater typically shows low salinity and reflects atmospheric or meteoric input before any significant geochemical evolution (Marandi & Shand, 2018; Gaikwad et al., 2022).

Figure 8 analyzes the hydrogeochemical processes using bivariate plots. An evaporation signature was observed in 9% of the data, where the Na^+/Cl^- ratio remained constant while electrical conductivity increased. This is consistent with the patterns described by Gaikwad et al. (2022) and Sangadi et al. (2022). Halite dissolution was identified in 14% of the samples, based on Na^+/Cl^- ratios close to unity (Figure 8A), while 28% showed $Na^+/Cl^- > 1.1$, suggesting cation exchange or silicate weathering. Fifty eight percent reported values < 0.90, which are indicative of reverse ion exchange (Askri et al., 2022). In Figure 8B, 86% of the data align with a slope of -0.98, supporting the significance of cation exchange reactions in groundwater mineralization (Abu-Alnaeem et al., 2018). Among these, 53% reflect reverse cation exchange, 36% reflect direct cation exchange, and the remaining 11% (although slightly offset) are likely to involve additional processes acting in synergy with ion exchange, such as silicate weathering (Gaikwad et al., 2022).

The salinization of aquifers by marine intrusion is commonly analyzed using the molar ratios of ions abundant in seawater, such as Cl^-, Mg^{2+}, and SO_4^{2-}. Among these, the $Cl^-/(HCO_3^-)$ ratio—also known as 'Simpson's ratio' (rS)— is widely applied because it effectively differentiates degrees of groundwater salinization associated with the influence of seawater (Abu-Alnaeem et al., 2018; Osiakwan et al., 2021). Based on rS values, the groundwater samples in this study were classified as follows: 16.50% correspond to uncontaminated water, 9.80% correspond to slightly contaminated water, 21.00% correspond to moderately contaminated water, 14.20% correspond to seriously contaminated water, and 38.70% correspond to highly contaminated water (Figure 8C).

The integrated analysis of bivariate plots, hydrogeochemical diagrams, and multivariate statistical methods provides a comprehensive framework for understanding the sources and geochemical processes governing groundwater chemistry in the Lower Sinú region.

The Na^+/Cl^- vs. EC relationship has been associated with anthropogenic sources of contamination, particularly when values fall below unity and coincide with brine zones in the Gibbs diagram (Abu-Alnaeem et al., 2018; Fernández-Martínez et al., 2019; El Yousfi et al., 2022). In the study area, the seasonal application of chlorinated fertilizers, such as potassium chloride (KCl), diammonium phosphate (DAP) and urea, during transitional seasons promotes chloride leaching and potassium fixation, contributing to elevated groundwater mineralization (Balasubramanian et al., 2022). Seventy two percent of brines belong to Group 2, where a strong positive Na^+-Cl^- correlation indicates simultaneous chloride enrichment and sodium depletion, probably via reverse ion exchange (Moussaoui et al., 2023).

Lithological influences are evident in the ($Ca^{2+} + Mg^{2+} - HCO_3^- - SO_4^{2-}$) vs ($Na^+ + K^+ - Cl^-$) and ($Na^+/Cl^-$ vs EC) binary plots and are further corroborated by the Gibbs, Chadha and Piper diagrams. Cation exchange driven salinization was observed in 4.4% (Chadha) and 4.0% (Gibbs) of the samples, while freshening through reverse cation exchange was indicated in 34.0% (Chadha), 18.8% (Piper), and 17.0% (Gibbs) of the samples. These findings are consistent with the water/rock interaction processes also highlighted in the Gibbs plot (7%).

The composition of the alluvial deposits—rich in plagioclases, micas, vermiculite-type clays, and montmorillonites—confirms a lithological source of the cations (IGAC, 2009). Sodium removal is attributed to reverse cation exchange with Ca^{2+} and Mg^{2+} (Osiakwan et al., 2021; Moussaoui et al., 2023), while the Na^+ inputs result from halite dissolution (7.5%) and evaporation concentration (9%). The weak to moderate correlations among Ca^{2+}, Mg^{2+}, SO_4^{2-}, and HCO_3^- support the inference that evaporite dissolution from calcite, gypsum, and dolomite is a minor contributor (Das et al., 2022).

Ca^{2+} and Mg^{2+} derive from both marine and lithological origins. Positive associations with Cl^- confirm a marine influence, while binary plot trends and mineralogical data

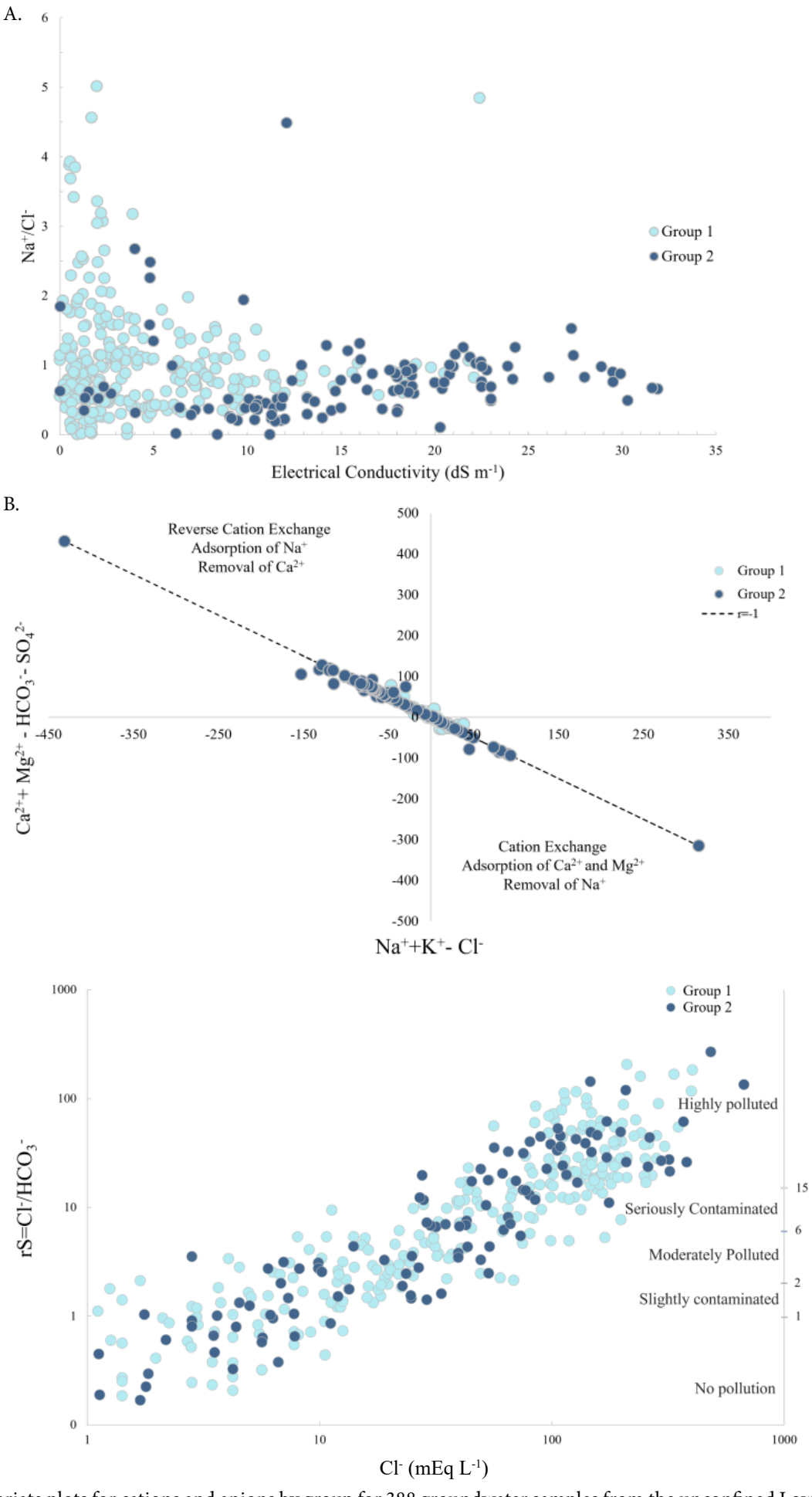

Figure 8. Bivariate plots for cations and anions by group for 388 groundwater samples from the unconfined Lower Sinú aquifer

indicate lithological sources (IGAC, 2009; Sangadi et al., 2022). High magnesium concentrations in the hydrogeological system contribute significantly to groundwater freshening, particularly through ion exchange processes (Osiakwan et al., 2021; Sangadi et al., 2022).

Sulfate, the second most abundant anion, probably originates from marine aerosols, especially in samples linked to meteoric recharge (Osiakwan et al., 2021; Balasubramanian et al., 2022). Moderate to weak positive correlations between sulfates, EC, marine ions, and TDS, along with weak inverse associations with pH, suggest that part of the sulfate could be used by organic matter, contributing to bicarbonate formation in the soil during wet and transitional seasons (Salem et al., 2021). Bicarbonate remains the least concentrated anion; weak correlations with EC, TDS, and major ions imply limited contributions from pedogenic or meteoric inputs (Salem et al., 2021).

Groundwater salinity and the concentration of marine-derived ions, such as Cl^-, Na^+, Mg^{2+}, and Ca^{2+}, commonly increase near coastal zones (Fernández-Martínez et al., 2019; El Yousfi et al., 2022). However, in the Lower Sinú region, correlations between these ions and the distance to the coastline were weak, indicating that proximity to the sea and the mechanism of marine intrusion do not fully explain the spatial patterns of groundwater salinization alone, as had been previously suggested for this sector of the Caribbean (Bustamante-Barrera & Cantero-Benitez, 2006; Narváez et al., 2014; Combatt et al., 2015).

Conclusions

1. The unconfined aquifer of the Lower Sinú receives salinizing ions from marine origin, lithological contributions, and agricultural sources.

2. Hydrogeochemical facies and multivariate analysis confirm that seawater intrusion and cation exchange are the main mineralization processes.

3. Hyperchlorinated brines in inland piezometers indicate significant contamination associated with agricultural activities.

4. Freshwater facies identified near the delta zone reflect meteoric recharge and limited geochemical evolution.

Contribution of authors: Zoraya Y. Martínez: formal analysis, writing, methodology, literature review and investigation; Adriana S. Raciny, Neider A. Burgos, Angela I. Villalba: data collection, writing—original draft preparation, data curation, literature review and investigation; Mónica C. Cantero, provided the data, writing—review and editing the manuscript, investigation and supervision of the work. All authors have read and agreed to the published version of the manuscript.

Supplementary documents: There are no supplementary sources.

Conflict of interest: The authors declare no conflicts of interest.

Financing statement: There is no funding to declare.

Acknowledgments: We extend our sincere thanks to the Universidad de Córdoba, Colombia, and to former professors Ivan Bustamante and Hermes Aramendis.

Literature Cited

Abu-Alnaeem, M. F.; Yusoff, I.; Ng, T. F.; Alias, Y.; Raksmey, M. Assessment of groundwater salinity and quality in Gaza coastal aquifer, Gaza Strip, Palestine: An integrated statistical, geostatistical and hydrogeochemical approaches study. Science of the Total Environment, v.615, p.972-989, 2018. https://doi.org/10.1016/j.scitotenv.2017.09.320

Askri, B.; Ahmed, A. T.; Bouhlila, R. Origins and processes of groundwater salinisation in Barka coastal aquifer, Sultanate of Oman. Physics and Chemistry of the Earth, v.126, e103116, 2022. https://doi.org/10.1016/j.pce.2022.103116

Balasubramanian, M.; Sridhar, S. G. D.; Ayyamperumal, R.; Karuppannan, S.; Gopalakrishnan, G.; Chakraborty, M.; Huang, X. Isotopic signatures, hydrochemical and multivariate statistical analysis of seawater intrusion in the coastal aquifers of Chennai and Tiruvallur District, Tamil Nadu, India. Marine Pollution Bulletin, v.174, e113232, 2022. https://doi.org/10.1016/j.marpolbul.2021.113232

Bauer, J.; Börsig, N.; Pham, V. C.; Hoan, T. V.; Nguyen, H. T.; Norra, S. Geochemistry and evolution of groundwater resources in the context of salinization and freshening in the southernmost Mekong Delta, Vietnam. Journal of Hydrology: Regional Studies, v.40, e101010, 2022. https://doi.org/10.1016/j.ejrh.2022.101010

Bustamante-Barrera, I. D.; Cantero-Benítez, M. C. Análisis de frecuencia e intensidad de eventos de inundación anual del Río Sinú, en el tramo La Doctrina-Boca de Tinajones, Córdoba Colombia antes y después del llenado y puesta en operación del embalse de la hidroeléctrica Urrá I y su impacto sobre los suelos. Suelos Ecuatoriales, v.36, p.77-82, 2006.

Combatt, C. E.; Narváez, M. H.; Bustamante-Barrera, I. D. Estimación de la salinidad en aguas freáticas del área de influencia de la desembocadura del río Sinú-Córdoba, Colombia. Idesia, v.33, p.55-63, 2015. https://doi.org/10.4067/S0718-34292015000300009

Das, C. R.; Das, S.; Panda, S. Groundwater quality monitoring by correlation, regression and hierarchical clustering analyses using WQI and PAST tools. Groundwater for Sustainable Development, v.16, e100708, 2022. https://doi.org/10.1016/j.gsd.2021.100708

El Yousfi, Y.; Himi, M.; El Ouarghi, H.; Elgettafi, M.; Benyoussef, S.; Gueddari, H.; Aqnouy, M.; Salhi, A.; Alitane, A. Hydrogeochemical and statistical approach to characterize groundwater salinity in the Ghiss-Nekkor coastal aquifers in the Al Hoceima province, Morocco. Groundwater for Sustainable Development, v.19, e100818, 2022. https://doi.org/10.1016/j.gsd.2022.100818

Fernández-Martínez, M.; Margalef, O.; Sayol, F.; Asensio, D.; Bagaria, G.; Corbera, J.; Sabater, F.; Domene, X.; Preece, C. Sea spray influences water chemical composition of Mediterranean semi-natural springs. Catena, v.173, p.414-423, 2019. https://doi.org/10.1016/j.catena.2018.10.035

François, H.; Le, S.; Pagès, J. Exploratory multivariate analysis by example using R. 2.ed. Boca Raton: CRC Press, 2017. 262p.

Gaikwad, S. K.; Gaikwad, S. P.; Wagh, V. M.; Meshram, D. C.; Kadam, A. K.; Muley, A. A.; Sahu, U. L. Appraisal of groundwater from lithological diversity of the western coastal part, Maharashtra, India: An integrated hydrogeochemical, geospatial and statistical approaches. Marine Pollution Bulletin, v.178, e113595, 2022. https://doi.org/10.1016/j.marpolbul.2022.113595

González-Pedraza, A. F.; Chiquillo-Barrios, Y. A.; Escalante, J. C. Soil salinization in agricultural areas of the Caribbean region and agroecological recovery strategies. Review. Inge CUC, v.18, p.14-26, 2022. http://doi.org/10.17981/ingecuc.18.1.2022.02

IGAC - Instituto Geográfico Agustín Codazzi. Métodos analíticos del laboratorio de suelos. Bogotá: IGAC, 2006. 648p.

IGAC - Instituto Geográfico de Agustín Codazzi. Estudio general de suelos y zonificación de tierras del departamento de Córdoba. Bogotá: IGAC, 2009. Available on: Available on: < https://metadatos.icde.gov.co/geonetwork/srv/api/records/14138630 >. Accessed on: Sept. 2024.

INGEOMINAS - Instituto Colombiano de Geología y Minería. Mapa hidrogeológico de Córdoba. Bogotá: INGEOMINAS, 2004. Available on: < https://catalogo.sgc.gov.co/cgi-bin/kpoha/opac-detail.pl?biblionumber=48448 >. Accessed on: Jun 2023.

Kelly, D. Development of seawater intrusion protection regulations. In: SWIM 19 - Proceedings of the 19th Salt Water Intrusion Meeting; 2006; Cagliari, Italy. p.135-146. Available from: < https://www.swim-site.nl/pdf/swim19/pages_135_146.pdf >. Accessed on: Jun. 2023.

Marandi, A.; Shand, P. Groundwater chemistry and the Gibbs Diagram. Applied Geochemistry, v.97, p.209-212, 2018. https://doi.org/10.1016/j.apgeochem.2018.07.009

Mercado-Fernández, T.; Ortega-Escobar, M.; Arenas-Tawil, A.; Combatt-Caballero, E. Dinámica de sales en el distrito de riego La Doctrina, Colombia. Idesia, v.29, p.83-90, 2011. https://doi.org/10.4067/s0718-34292011000100011

Moussaoui, I.; Rosa, E.; Cloutier, V.; Neculita, C. M.; Dassi L. Chemical and isotopic evaluation of groundwater salinization processes in the Djebeniana coastal aquifer, Tunisia. Applied Geochemistry. v.149, e105555, 2023. https://doi.org/10.1016/j.apgeochem.2022.105555

Narváez, M. H.; Combatt, C. E.; Bustamante-Barrera, I. Distribución espacial de la salinidad en suelos del área de influencia de la desembocadura del río Sinú. UDCA Actualidad & Divulgación Científica, v.17, p.433-443, 2014. http://www.scielo.org.co/scielo.php?pid=S0123-42262014000200014&script=sci_arttext

Osiakwan, G. M.; Appiah-Adjei, E. K.; Kabo-Bah, A. T.; Gibrilla, A.; Anornu, G. Assessment of groundwater quality and the controlling factors in coastal aquifers of Ghana: An integrated statistical, geostatistical and hydrogeochemical approach. Journal of African Earth Sciences, v.184, e104371, 2021. https://doi.org/10.1016/j.jafrearsci.2021.104371

Richards, L. A. Diagnosis and improvement of saline and alkali soils. Washington, DC: U.S. Department of Agriculture; 1954. 160p. Agriculture Handbook No. 60

Salem, Z. E. S.; Abdelrahman, K.; Kováčiková, S.; Badran, O. M. Use of various statistical techniques to assess the vertical and lateral change in the groundwater chemistry of Quaternary aquifer in an irrigated highly populated area. Journal of King Saud University Science, v.33, e101556, 2021. https://doi.org/10.1016/j.jksus.2021.101556

Sangadi, P.; Kuppan, C.; Ravinathan, P. Effect of hydro-geochemical processes and saltwater intrusion on groundwater quality and irrigational suitability assessed by geo-statistical techniques in coastal region of eastern Andhra Pradesh, India. Marine Pollution Bulletin, v.175, e113390, 2022. https://doi.org/10.1016/j.marpolbul.2022.113390

Sunkari, E. D.; Seidu, J.; Ewusi, A. Hydrogeochemical evolution and assessment of groundwater quality in the Togo and Dahomeyan aquifers, Greater Accra Region, Ghana. Environmental Research, v.208, e112679, 2022. https://doi.org/10.1016/j.envres.2022.112679

Tajwar, M.; Rahman, M.; Hasan, M.; Sakib, N.; Shreyad, S. S.; Alam, M. M. T.; Gazi, M. Y.; Hoque, S. A.; Zahid, A. Interpreting hydrogeochemical interactions and controlling processes in groundwater using advanced statistical techniques in the Southeast Asian megacity: Dhaka, Bangladesh. Cleaner Water, v.7, e100084, 2025. https://doi.org/10.1016/j.clwat.2025.100084

Telahigue, F.; Souid, F.; Agoubi, B.; Chahlaoui, A. Hydrogeochemical and isotopic evidence of groundwater salinization in a coastal aquifer: A case study in Jerba Island, southeastern Tunisia. Physics and Chemistry of the Earth, v.118-119, e102886, 2020. https://doi.org/10.1016/j.pce.2020.102886

Torres-Bejarano, F.; González-Martínez, J.; Rodríguez-Cuevas, C.; Mathis, T. J.; Rodríguez-Pérez, J.; Tran, D. K. Characterization of salt wedge intrusion process in a geographically complex microtidal deltaic estuarine system. Journal of South American Earth Sciences, v.131, e104646, 2023. https://doi.org/10.1016/j.jsames.2023.104646

Wang, H.; Yang, Q.; Liang, J. Interpreting the salinization and hydrogeochemical characteristics of groundwater in Dongshan Island, China. Marine Pollution Bulletin, v.178, e113634, 2022. https://doi.org/10.1016/j.marpolbul.2022.113634

Xu, X.; Xiong, G.; Chen, G.; Fu, T.; Yu, H.; Wu, J.; Liu, W.; Su, Q.; Wang, Y.; Liu, S.; Shi, X. Characteristics of coastal aquifer contamination by seawater intrusion and anthropogenic activities in the coastal areas of the Bohai Sea, eastern China. Journal of Asian Earth Sciences, v.217, e104830, 2021. https://doi.org/10.1016/j.jseaes.2021.104830